

**₁ A Divide and Conquer Approach to Cope with
₂ Uncertainty, Human Health Risk and Decision
₃ Making in Contaminant Hydrology**

Felipe P. J. de Barros¹, Diogo Bolster², Xavier Sanchez-Vila³ and Wolfgang
Nowak⁴

F.P.J. de Barros, Institute of Applied Analysis and Numerical Simulation/SimTech, Pfaffen-
waldring 57, University of Stuttgart, 70569 Stuttgart, Germany. (felipe.debarros@simtech.uni-
stuttgart.de)

¹Institute of Applied Analysis and

4 **Abstract.** Assessing health risk in hydrological systems is an interdis-
5 ciplinary field. It relies on the expertise in fields of hydrology and public health
6 and needs powerful translation concepts to provide decision support and pol-
7 icy making. Reliable health risk estimates need to account for the uncertain-
8 ties and variabilities present in hydrological, physiological and human be-
9 havioral parameters. Despite significant theoretical advancements in stochas-
10 tic hydrology, there is still a dire need to further propagate these concepts
11 to practical problems and to society in general. Following a recent line of work,

Numerical Simulation/SimTech,

Pfaffenwaldring 57, University of Stuttgart,

70569 Stuttgart, Germany

²Environmental Fluid Dynamics

Laboratories, Dept. of Civil Engineering

and Geological Sciences, University of Notre

Dame, IN 46556, USA.

³Dept. of Geotechnical Engineering and

Geosciences, Technical University of

Catalonia, E-08034 Barcelona, Spain.

⁴Institute of Hydraulic Engineering,

LH²/SimTech, University of Stuttgart,

Pfaffenwaldring 61, 70569 Stuttgart,

Germany.

12 we use of fault trees to address the task of probabilistic risk analysis (PRA)
13 and to support related decision and management problems. Fault trees al-
14 low to decompose the assessment of health risk into individual manageable
15 modules, thus tackling a complex system by a structural divide and conquer
16 approach. The complexity within inside each module can be chosen individ-
17 ually according to data availability, parsimony, relative importance and stage
18 of analysis. Three differences are highlighted in the current paper when com-
19 pared to previous works: (1) The fault tree proposed here accounts for the
20 uncertainty in both hydrological and health components, (2) system failure
21 within the fault tree is defined in terms of risk being above a threshold value
22 whereas previous studies that used fault trees used auxiliary events such as
23 exceedance of critical concentration levels and (3) we introduce a new form
24 of stochastic fault tree that allows to weaken the assumption of independent
25 subsystems that is required by a classical fault tree approach. We illustrate
26 our concept in a simple groundwater-related setting.

1. Introduction

27 Assessing the impact of water pollutants on human health relies on our ability to accu-
28 rately assess two things: first, the transport and possible reactions between contaminants
29 in a hydrosystem and second, evaluating the physiological response of humans to such
30 contaminants and the resulting adverse effects on human health [e.g., *Andricevic and*
31 *Cvetkovic*, 1996; *Maxwell et al.*, 1998; *Maxwell and Kastenberg*, 1999; *Maxwell et al.*,
32 1999; *Benekos et al.*, 2007; *de Barros and Rubin*, 2008; *Maxwell et al.*, 2008]. Notori-
33 ously, both of these fields contain uncertainty for a variety of reasons. These include
34 the lack of characterization data, inadequate conceptual models and the occurrence of
35 natural variability in both hydrosystems and health components [*Bogen and Spear*, 1987;
36 *McKone and Bogen*, 1991; *Burmester and Wilson*, 1996; *Maxwell and Kastenberg*, 1999].
37 Given such uncertainties, following the traditional route of making single deterministic
38 predictions for a given scenario has little practical purpose [*USEPA*, 2001]. This fact has
39 been recognized in recent times by many large-scale government regulatory bodies. As a
40 consequence, they increasingly insist on the use of probabilistic approaches that include
41 estimates in uncertainty of risk [e.g., *Rubin et al.*, 1994; *Andricevic and Cvetkovic*, 1996;
42 *Davison et al.*, 2005; *Persson and Destouni*, 2009].

43 In an ideal world with extensive computational resources, one might try to tackle
44 such water-related health impact problems in a probabilistic framework by running high-
45 resolution Monte-Carlo simulations of the entire interacting system at full complexity.
46 However, the multi-component (and multi-scale) nature of these problems can often ren-
47 der such an approach difficult (if not impossible) to implement in practice. On the hy-

48 drological side of the problem, heterogeneity in many physical and chemical parameters
49 can range over multiple orders of magnitude and lead to scale-dependence of process de-
50 scriptions. Depending on the specific problem at hand and the contaminants in question,
51 the number of required parameters can be very large, far beyond parsimony, with lim-
52 ited spatial resolution of the hydrosystem [Rubin, 2003; Tartakovsky and Winter, 2008].
53 Similarly, on the health side, natural variability in human behavior, age, body type and
54 genetic characteristics (to mention but a few) lead to large variability in physiological
55 parameters [e.g., Maxwell and Kastenber, 1999].

56 Apart from the unresolved issues with natural variability that occur in both parts of
57 the system, it is not even entirely clear that the conceptual mathematical models used in
58 each field are fully appropriate. For example, in hydrogeology, there is an ever increasing
59 number of field, laboratory and numerical data sets, indicating that “anomalous” behavior
60 (i.e. non-Fickian phenomena that cannot be described by the traditional advection dis-
61 persion equation approaches) may in fact not be all that anomalous but rather the rule
62 [e.g., Gelhar et al., 1992; Sidle et al., 1998; Silliman et al., 1997; Levy and Berkowitz,
63 2003; Fiori et al., 2007]. Such anomalies, observed in conservative transport, pose even
64 further complications for the transport of reactive solutes [Raje and Kapoor, 2000; Gram-
65 ling et al., 2002]. However, there is a continuous emergence of new models that appear
66 capable of capturing these effects [e.g., Neuman and Tartakovsky, 2009; Benson and Meer-
67 schaert, 2008; Donado et al., 2009; Bolster et al., 2010; Ederly et al., 2009]. On the health
68 side, many of the mathematical dose-response models rely on linear extrapolation of data
69 from high-dose laboratory experiments on animals [Fjeld et al., 2007], which do not take
70 into account the possibility of nonlinear behavior at lower doses [Bogen and Spear, 1987;

71 *McKone and Bogen, 1991; Burmaster and Wilson, 1996*]. In response to these limitations
72 and uncertainties on both sides of the problem, a recent series of papers has emerged that
73 quantified the relative gain in overall information from enhanced characterization in each
74 component in probabilistic health risk assessment [*de Barros and Rubin, 2008; de Barros*
75 *et al., 2009*].

76 As with many applied sciences and engineering disciplines, the correct implementation
77 of assessing health-related risk in hydrosystems is an interdisciplinary field. It relies on
78 the expertise of hydrologists and physiologists/toxicologists as well as a potentially large
79 number of other disciplines, depending on the specific problem being considered. Addi-
80 tionally, in practical situations, stakeholders (e.g. managers, politicians, judges etc.), who
81 are given the responsibility of making decisions within such complex systems, are typi-
82 cally only experts in one field at most. As a result, there is a strong need to communicate
83 information across interfaces between different fields in an efficient and comprehensible
84 manner, which is rarely an easy task [*McLucas, 2003*]. For example, despite significant
85 theoretical advancements in stochastic hydrogeology over the last several decades, stronger
86 efforts are still needed to transfer this knowledge to applications [see discussions in *Rubin,*
87 *2003; Christakos, 2004; Freeze, 2004; Rubin, 2004; Pappenberger and Beven, 2006*].

2. Goals, Approach and Contribution

88 In this work, we propose a formal probabilistic risk analysis (PRA) that relies on the use
89 of fault trees and can address all of the above mentioned issues. Fault trees have commonly
90 been used in risk assessment concerning engineered systems [e.g., *Bedford and Cooke,*
91 *2003*]. However, for a variety of reasons, e.g., because hydrosystems are comprised of a
92 mixture of natural and engineered components that complicates matters, this approach

93 has been receiving increasing attention in the hydrological community [*Tartakovsky*, 2007;
94 *Winter and Tartakovsky*, 2008; *Bolster et al.*, 2009]. The basic idea of this methodology is
95 simple and can be summarized as a divide and conquer approach: It consists of taking a
96 large and complex system that is difficult to handle and dividing it into a series of quasi-
97 independent simpler systems (modules) that are manageable on an individual scale. Once
98 each of the smaller problems has been addressed, they can be recombined in a systematic
99 manner to look at the large system. According to *Bedford and Cooke* [2003], a rigorous
100 PRA based on fault tree should consist of the following steps:

- 101 1. Define failure of the system to be examined, where system failure must be defined a
102 priori by stakeholders.
- 103 2. Identify the key components of the system and all events that must occur for the
104 system to fail.
- 105 3. Construct a fault tree that visually depicts the combination of these events.
- 106 4. Develop a mathematical representation of the fault tree by the use of Boolean alge-
107 bra.
- 108 5. Compute the probabilities of occurrence of each event.
- 109 6. Use these to calculate the probability of failure for the entire system.

110 The advantages of the divide and conquer approach is that, for a well developed fault
111 tree, each key component/event should be quasi-independent from all others (i.e., if there
112 is a dependence it should be weak). Therefore, each event can be tackled without explicit
113 knowledge of all others. For example, in *Bolster et al.* [2009], each of the events was
114 studied by a different person without mutual interaction. This opens the gateway for

115 interdisciplinary cooperation, as each component can be addressed independently by the
116 most appropriate expert.

117 Additionally, a decision maker can use the fault tree to visually understand where risk
118 and uncertainty emerge from in this system, without having to enter into the complex
119 details of each component. In some sense, the fault tree acts as a translator of information
120 between experts in different fields, thus enabling better decision making.

121 Another benefit of such a fault tree approach is that one can work with each individ-
122 ual component: For instance, one can replace the method of examining each component
123 without having to touch the others. This can be thought of as analogous to the object-
124 oriented approach to programming, where one only updates the necessary objects as the
125 demand arises without having to rewrite an entire code. This enables better allocation
126 of resources and incorporation of more advanced theories and data sets as they become
127 available. For example, as a starting point one can use simple calculations to study each
128 component. With such an initial estimate, one can identify the events which contribute
129 most to the final risk or those which propagate the highest degree of uncertainty through
130 the system. This information can be used to allocate further resources to these dominant
131 events, and more sophisticated and detailed models can be pursued for these events as new
132 data or advanced theoretical models become available. Moreover, it can be use towards
133 rational allocation of resources for further data acquisition [*de Barros et al.*, 2009; *Nowak*
134 *et al.*, 2010] within a dynamical and adaptive framework. Thus, fault trees can struc-
135 ture and guide through the entire process of PRA, from initial screening over additional
136 investigations and refinement to the final conception of risk management strategies.

137 The purpose of this work is to extend the fault tree framework used by *Bolster et al.*
138 [2009] to account for both hydrology and human physiological/behavioral characteristics.
139 We develop this idea by unifying the framework provided by *Bolster et al.* [2009] with the
140 ideas of *Maxwell and Kastenber* [1999], *Maxwell et al.* [1999] and *de Barros and Rubin*
141 [2008]. *Bolster et al.* [2009] defined system failure by exceeding a regulatory threshold
142 concentration. In contrast, we define the ultimate prediction goal (i.e., human health
143 risk) to be the center of attention, and define system failure as exceeding a threshold
144 risk value [as done in *Maxwell and Kastenber*, 1999]. Such threshold risk is often given
145 by environmental regulation bodies for the sensitive target at stake [e.g., *USEPA*, 2001].
146 The novelty here lies in constructing a fault tree analysis that includes the uncertainty
147 and variability from both hydrological and human health risk parameters. One of the
148 new key features of this choice is that it allows us to investigate the role of health-related
149 variability and uncertainty in decision making. For instance, if the concentration value at
150 a drinking water supply is higher than that allowed, but if the characteristics of exposed
151 individuals are such that little of that contamination is ingested or metabolized, then
152 individuals might be at little or no risk.

153 We begin by defining the problem formulation and presenting a generic methodology
154 for developing fault trees in hydrological systems. More precisely, we propose a stochastic
155 fault tree method. To elucidate this process and demonstrate its strengths, we present a
156 specific illustrative example. We consider a simple groundwater contamination scenario,
157 illustrating how system failure and related uncertainty therein changes (i) according to
158 the physical characteristics of the flow and transport problem and (ii) for different levels
159 of uncertainty and variability in the health component.

3. Problem Formulation

3.1. The Co-Existence of Water-Related Health Hazards

160 Surface or groundwater can be polluted by the presence of many different chemicals
161 (either organic or inorganic) as well as pathogenic microorganisms (bacteria, protozoa,
162 and viruses) [e.g, *Molin and Cvetkovic*, 2010]. Exposure of humans to polluted water
163 through ingestion, inhalation, or skin contact may produce a number of different diseases.
164 Whether one of these potential diseases is developed in a given individual depends on the
165 toxicity of the pollutant, but also on the metabolism, personal habits of an individual's
166 water-related practices and finally, consumption and exposure habits.

167 Diseases can be either caused by accumulation over the years or by acute exposure,
168 i.e., over a very short period of time. Synergetic effects may cause the same pollutant to
169 have different toxicity in different parts of the world; e.g., lung cancer may be caused by
170 drinking water with a high concentration of trihalomethanes, but it is also likely to be
171 developed in people living in areas with heavy atmospheric pollution.

Obviously, for a given hazardous substance when either concentration or time of exposure increases, so does the potential (risk) of developing a disease. Actual existing models are highly disputable, since most of them are extrapolations from high-dose laboratory experiments carried out on animals such as mice to low-dose effects on humans [e.g., *McKone and Bogen*, 1991]. We denote $r_i(x, t), i = 1..N$, as the risk associated to the development of a given adverse health effect for a given pollutant, N being the number of chemicals released. In general, r_i are supposed to be small values (otherwise the problem is considered pandemic). Thus, the potential development of two or more diseases at exactly the same time can be considered negligible, and total risk can be taken as the sum

of the individual risks:

$$r(x, t) = \sum_{i=1}^N r_i(x, t). \quad (1)$$

3.2. Evaluating Health Risk for a Particular Substance and Exposure Pathway

The starting point for this section is to formulate human health risk for a single substance i in probabilistic terms following *de Barros and Rubin* [2008]. Depending on the particular contaminant, there are a number of models to evaluate the risk [*Maxwell and Kastenber*, 1999; *Morales et al.*, 2000; *Fjeld et al.*, 2007; *de Barros et al.*, 2009; *Molin et al.*, 2010].

In order to simplify the discussion, let us consider a carcinogenic contaminant. The increased lifetime cancer risk r due to the groundwater ingestion pathway (chronic exposure) for an individual is expressed by an assumed linear model as [*USEPA*, 1989]:

$$r(\mathbf{x}, \mathbf{t}) = \beta C(\mathbf{x}, \mathbf{t}), \quad (2)$$

where concentration $C(\mathbf{x}, t)$ [mg/l] is an outcome of all the relevant flow, transport and transformation processes in the system at hand. β is a lumped parameter that accounts for all the behavioral and physiological parameters:

$$\beta = \frac{IR \times ED \times EF}{BW \times AT} \times Sf_o, \quad (3)$$

where IR [l/d] denotes the ingestion rate, ED [y] represents exposure duration, EF [d/y] is the exposure frequency, BW [kg] is the body weight, AT [d] is the average time, and Sf_o is the slope factor [kg-d/mg], obtained from experiments. Note that C can represent a point concentration or a flux-averaged concentration. In most health risk applications, C corresponds either to the peak concentration or to an averaged concentration over the

185 exposure period at a environmentally sensitive target [see *Maxwell and Kastenber*, 1999].
 186 All the health parameters are values corresponding to an individual from the exposed
 187 population. These parameters contain some level of uncertainty and vary from individual
 188 to individual [*Dawoud and Purucker*, 1996]. A large degree of uncertainty is present in Sf_o
 189 because of the animal to human extrapolation [*McKone and Bogen*, 1991]. Expression
 190 (2) is merely a simplification of a more general model that includes several exposure
 191 pathways, contaminant dependencies and non-linearities [*Maxwell and Kastenber*, 1999;
 192 *Morales et al.*, 2000; *Fjeld et al.*, 2007; *de Barros et al.*, 2009]:

$$r(\mathbf{x}, \mathbf{t}) = \beta_G[C(\mathbf{x}, \mathbf{t}) - C_G^*]^{m_G} + \beta_H[C(\mathbf{x}, \mathbf{t}) - C_H^*]^{m_H} + \beta_S[C(\mathbf{x}, \mathbf{t}) - C_S^*]^{m_S}, \quad (4)$$

193 where the subscripts G stands for ingestion, H for inhalation, and S for contact through
 194 skin and β_j are coefficients that relate to the toxicities of the substance for each pathway.
 195 C_j^* is the corresponding threshold value, i.e., a value below which we do not expect any
 196 adverse effects for an individual. These threshold values are pollutant dependent. The
 197 exponents m_G , m_H and m_S determine the non-linearity of each dose-response curve [*Fjeld*
 198 *et al.*, 2007]. In the case of carcinogenic compounds, USEPA suggests to use a zero value.
 199 This indicates that, no matter how small the concentration is in water, risk is never null
 200 [*USEPA*, 1989, 1991]. An alternative is using the detection limit given by the chemical
 201 analytical method. Equation (4) can only be used if each individual term C_j is above C_j^* ;
 202 otherwise the individual term should be removed from the equation.

203 For the sake of discussion but without loss of generality, we will work with the model
 204 expressed in equation (2) to demonstrate the modular character of the methodology pro-
 205 posed. It will serve to illustrate the purpose and exchange character of the suggested

206 methodology. Still, at any time, more complex risk models, such as Eq. (4) can be incor-
207 porated. The only prerequisite is that sufficient data should be available to justify any
208 more complex choice (see works by *Troldborg et al.* [2008, 2009]) .

3.3. Stochastic Representation of Human Health Risk

209 According to Eq. (2), risk is the product of two quantities, both of them uncertain.
210 Uncertainty in β comes from the imperfect characterization (and lack of knowledge) of
211 the toxicity. However, β is also variable since its value varies from individual to individual
212 within the exposed population. Values of β also vary according to the population cohort
213 such as age groups and gender [*Yu et al.*, 2003; *Maddalena and McKone*, 2002]. *Maxwell*
214 *et al.* [1998] and *Maxwell and Kastenber* [1999] reported that the impact of the variability
215 in β on risk is very significant.

216 The remaining issue is to evaluate the contaminant concentration at any particular point
217 within an environmentally sensitive target (Ω_p) over a period of time t_p , $C(\mathbf{x} \in \Omega_p, t_p)$ and
218 to quantify its uncertainty. Spatial variability and uncertainty in concentration is due to
219 the ubiquitous heterogeneity in physical and biochemical processes, boundary conditions
220 and contaminant release patterns. The processes involved are solute- and soil-dependent,
221 and might include advection, diffusion, dispersion, sorption, precipitation/dissolution,
222 redox processes, cation exchange, evaporation/condensation, microbial or chemical trans-
223 formation and decay. For any given substance, an appropriate model is written as a
224 governing equation that depends on a number of parameters. In most applications, there
225 is a need to be careful with the problem of scales, since both the relevant processes as
226 well as the representative parameters are often scale dependent.

227 Accepting that $C(\mathbf{x} \in \Omega_p, t_p)$ and β are uncertain, the resulting risk r is regarded as
 228 a random function R , with a cumulative distribution function (cdf) $F_R(r) = Pr(R \leq r)$.
 229 Thus, it is convenient to formulate risk in terms of exceeding probabilities [e.g., *Andricevic*
 230 *and Cvetkovic*, 1996; *de Barros and Rubin*, 2008]:

$$Pr(R > r_{crit}) = 1 - F_R(r_{crit}), \quad (5)$$

231 with r_{crit} representing an environmentally regulated value, for instance, $r_{crit} = 10^{-6}$ or
 232 10^{-4} [*USEPA*, 1989].

233 Uncertainty in the concentration can be reduced by conditioning on measurements of
 234 either the dependent variables (e.g. concentrations, groundwater heads, river discharges,
 235 etc) or the parameters themselves (through field or laboratory tests). Details concerning
 236 different mentalities on uncertainty reduction through conditioning can be found in the
 237 literature [e.g., *Rubin*, 1991; *Kitanidis*, 1995; *Bellin and Rubin*, 1996; *Freer et al.*, 1996;
 238 *Zimmerman et al.*, 1998]. Once it is decided which components to investigate in more
 239 detail, specific methods for optimal experimental design can be used, e.g., for optimal
 240 sampling layouts [e.g., *Ucinski*, 2005; *Nowak et al.*, 2010; *Nowak*, 2010].

4. Methodology: Fault-Tree Analysis

241 Before one can begin any fault tree analysis, one must define the system that is being
 242 investigated. The system that we consider in this work is depicted schematically in Figure
 243 1. This figure illustrates several sources of contamination (SO_i), a general mean flow field
 244 and a region that we define as the protection region (Ω_p). The sources of contamination
 245 could be anything from natural sources (e.g. arsenic), known spill sites, industrial regions
 246 where contamination of certain pollutants may be probable, or agricultural lands where

247 certain contaminants may occur, to any other imaginable source of contamination. Sim-
248 ilarly the protection zone could be anything like a well field, a lake or a residential area.
249 The system defined in this work is deliberately kept generic and would of course be made
250 more specific to a particular problem under consideration as the demand arises. Based
251 on this generic system, we will follow the six steps outlined in the introduction. We will
252 present a more specific illustrative example in the following section.

253 Step 1: Defining System Failure

254 We define failure of this system (SF) when risk, as defined in section 3, exceeds a critical
255 regulatory value:

$$SF : r > r_{crit} \quad (6)$$

256 with exceedance probability given by Eq (5).

257 Step 2: Identifying the Key Components/Events

258 We use this particular step to divide the problem into two components: A hydrologi-
259 cal contamination scenario and the consequences of contamination on human health risk.
260 This is an important distinction because concentration exceedance does not imply that
261 the population is at risk. For example, individuals not drinking tap water (or with ex-
262 ceptional physiology) might be at little or no risk. For such reasons, the combination of
263 the concentration and the health parameters is the important factor to consider (only the
264 joint effect can culminate in adverse health effects).

265 The first key component follows a similar path to the works of *Tartakovsky* [2007],
266 *Winter and Tartakovsky* [2008] and *Bolster et al.* [2009]. It focuses on the hydrological
267 component and is meant to establish whether it is necessary at all to consider health risk.
268 This event is called “Critical Concentration of Exposure ”(CCE_i) and is defined as the
269 event that the concentration of a contaminant i , arriving at the protection zone, exceeds
270 some critical concentration value. If such an event occurs, decision makers must be alerted
271 and should become concerned about the consequences on human health. The lower-level
272 events associated with this key event are:

273 \mathbf{SO}_i (Source Occurrence) is the event that a contaminant exists. In many possible
274 scenarios, the existence of a contaminant source is not deterministic. For instance, a
275 contamination source provenient from fertilizers or pesticides within an agricultural zone
276 may (or may not) exist and the probability of its occurrence must be quantified.

277 $\mathbf{P}_{1,i}$ (Plume Path 1) is the event that the plume evolving from contaminant source i
278 bypasses the protection zone.

279 $\mathbf{P}_{2,i}$ (Plume Path 2) refers to the event that the same plume hits the protection zone.
280 If such a path does not exist, due to the morphology of the hydrosystem, then there is no
281 reason for concern

282 \mathbf{NA}_i (Natural Attenuation) represents the event that natural attenuation can decrease
283 concentration peaks below a defined threshold value through chemical reactions, dispersion
284 and dilution.

285 The second component relates to all health risk considerations. For this component,
 286 the basic events are:

287 **CCE_i** (Critical Concentration of Exposure) reflects the concentration that, when com-
 288 bined to a value β (see the relation in Eq. 2), will result in risk exceeding its critical value
 289 established by regulations (e.g., $r_{crit} = 10^{-6}$ or 10^{-4}), i.e., system failure will occur.

290 **BPC_i** (Behavioral Physiological Component) corresponds to the event that an individ-
 291 ual (or population cohort) that is exposed has characteristic β (see Eq. 3).

292 The point to note here is that CCE_i is conditioned on a value of β provenient from
 293 BPC_i , which, as highlighted in section 3, is not a single value and it varies within the
 294 population based on several parameters [e.g., *Maxwell et al.*, 1998; *Maxwell and Kasten-*
 295 *berg*, 1999; *Maxwell et al.*, 1999; *de Barros and Rubin*, 2008; *de Barros et al.*, 2009]. As
 296 expressed in Equation (4), each individual contains a specific β (e.g., j^{th} individual with
 297 characteristic β_j). The fact that CCE_i can be defined only for a given value of β will re-
 298 quire, in a later stage of our analysis, an extension of the conventional fault tree approach
 299 to account for all possible values from the distribution of β .

300 **Step 3: Building the Fault Tree(s)**

301 In step 2, we divided the problem into two sections. In this step we will draw a fault tree
 302 for each of those sections. The first branch of the fault tree addresses the hydrogeological
 303 contamination scenario, leading to the key event CCE_i . The fault tree is shown in Figure
 304 2 and is, in some sense, a version of the fault tree discussed in *Bolster et al.* [2009]. The
 305 combination with the second branch yields the main fault tree and represents the novelty

306 of this work. This main fault tree replicates for each contaminant species and source and
 307 is shown in Figure 3. It illustrates visually how we have linked contamination and human
 308 health risk. The system failure (risk exceedance) for contaminant i is the joint occurrence
 309 of the events CCE_i and BPC_i .

310 Those readers who are familiar with fault trees might notice a particular gate (Boolean
 311 operator) below the R_{crit} event they are not familiar with. This gate is novel and we
 312 define it as an “ENSEMBLE AND” gate. It reflects the fact that the R_{crit} event must
 313 be calculated based on all possible values of β and of the concentration arriving at the
 314 protection zone. The ensemble operator $\langle \dots \rangle_\beta$ indicates that the averaging should be done
 315 over the ensemble of β to obtain the risk over the average individual because $Pr[R] =$
 316 $\langle Pr[R|\beta] \rangle_\beta$. The fault tree without the operator $\langle \dots \rangle_\beta$ would be equivalent to a tree
 317 for a single exposed individual with known characteristics and with known toxicity. In
 318 other words, the fault tree shown here is generalized for every individual of the exposed
 319 population. The fault tree depicted in Figure 3 allows us to evaluate system failure for an
 320 average individual over a specified population cohort (e.g., average senior with β specified
 321 over a range of possible values), average individual over all the exposed population (aver-
 322 aging over all β range) or for a single exposed individual (with specified β_j). This process
 323 represents the internal loop from the nested Monte Carlo approach proposed by *Maxwell*
 324 *and Kastenber* [1999]. *Maxwell et al.* [1998] and *Maxwell and Kastenber* [1999] showed
 325 how the variabilities within health parameters have a strong impact in human health risk
 326 prediction. As with all fault tree analysis, it is meant to act as a visual aid to the user to
 327 understand where risk can come from. Accounting for $\langle \dots \rangle_\beta$ within the fault tree implies
 328 that one needs to account for the variability in its description such that one can assign the

329 probability of occurrence for the event R_{crit} . The “ENSEMBLE AND” gate generalizes
 330 the previous fault tree by covering over all range of population behavioral characteristics.

331 Step 4: Translation to Boolean Logic

332 This part can be viewed as the final stage in the development of the risk assessment
 333 system. The subsequent steps (items 5 and 6 in the introduction) involve the actual
 334 calculations of probabilities of all basic events and the combination thereof based on
 335 the expression that emerges from the current step. First, we will write a Boolean logic
 336 expression for the probability of event CCE_i occurring. The “AND” and “OR” operators
 337 represents multiplications and additions of probabilities respectively. As discussed (and
 338 as can be seen from the fault tree in Figure 2), the appropriate Boolean expression for
 339 failure CCE_i is given by

$$CCE_i = SO_i \text{ AND } P_{2,i} \text{ AND } NA_i, \quad (7)$$

340 with probability of occurrence:

$$Pr[CCE_i] = Pr[SO_i] Pr[P_{2,i}] Pr[NA_i], \quad (8)$$

341 since SO_i , $P_{2,i}$ and NA_i are completely independent of each other. Similarly, for the main
 342 fault tree depicted in Figure 3, the Boolean expression for system failure associated with
 343 each source $R_{crit,i}$ can be written as

$$R_{crit,i} = CCE_i \text{ AND } BPC \quad (9)$$

344 with probability of occurrence:

$$Pr[R_{crit,i}] = Pr[CCE_i] Pr[BPC]. \quad (10)$$

345 If more contaminants are present ($i \geq 2$), then the total system failure (SF_{all}) is given
 346 by:

$$SF_{all} = R_{crit,1} \text{ OR } R_{crit,2} \text{ OR } \dots \text{ OR } R_{crit,N} \quad (11)$$

and the probability of system failure is given by

$$Pr[SF_{all}] = Pr[SF_1] + Pr[SF_2] + \dots + Pr[SF_N]. \quad (12)$$

347 Steps 5 and 6, see Section 2, are straightfoward and need no further explanation. In
 348 the following section, we will develop them for an illustrative example.

5. Illustrative Example

349 Our goal is to show how the methodology can accommodate the entire range from
 350 simple to complex problems and solution approaches. It is seldom that a large data
 351 set is available in probabilistic health risk assessment, and we cannot always solve the
 352 problem entirely. For such reasons, it is common to make conservative assumptions and
 353 assess the worst case scenario with simple models [*Trolldborg et al.*, 2009; *Bolster et al.*,
 354 2009]. The scenario under consideration assumes almost complete absence of site-specific
 355 data, leading to crude yet conservative estimates of probabilities. Other existing methods
 356 rather than the simple one we selected for the illustration here can be found in the
 357 literature, (e.g. see *Rubin* [2003] for an extensive review). The level of complexity in
 358 the analysis of each component and event can vary according to the available information
 359 and the importance within the fault tree, and can easily be adapted interactively during

360 the analysis. If hydrological field data is available and more complex physical-chemical
361 processes are involved, one may opt for numerical Monte Carlo simulations to allow more
362 flexibility in relaxing simplifying assumptions as done in *Maxwell and Kastenber* [1999];
363 *Maxwell et al.* [1999] and *de Barros et al.* [2009]. Without loss of generality, our illustrative
364 example will focus in a groundwater contamination problem. The method shown here can
365 also be applied to surface water bodies or to coupled catchment-scale problems [e.g.,
366 *Baresel and Destouni*, 2007; *Persson and Destouni*, 2009].

5.1. Physical Scenario and Assumptions

367 We consider a regional aquifer, confined, 2D depth-averaged with mean flow velocity
368 U taken along the x -direction. A degrading contaminant is continuously released with
369 inlet concentration C_o within a rectangular source with transverse dimension $w = y_{SR} -$
370 y_{SL} (see Figure 4). Once contamination has occurred, the contaminant plume might hit
371 the environmentally sensitive target represented by a control plane (CP) situated at a
372 distance $x = L_b - L_s$ from the source zone (see Figure 4). The schematic representation
373 of the physical problem is given in Figure 4.

374 At this stage, we will evaluate the concentration field under the worst case scenario.
375 This is a common approach in human health risk assessment since decision makers must
376 account for safety factors when dealing with human lives [*Troldborg et al.*, 2008, 2009;
377 *McKnight et al.*, 2010]. We assume, in accordance with the worst case scenario philosophy,
378 that the concentration can be calculated using a 1D solution by neglecting transverse
379 dispersion between neighboring streamlines. Further more, longitudinal dispersion is also
380 neglected. This excludes dilution processes as described by *Kitanidis* [1994]. The only

381 natural attenuating factor is degradation with linear decay coefficient λ (neglecting pore-
 382 scale dispersion):

$$C(\tau) = C_o \exp[-\lambda\tau], \quad (13)$$

383 where $\tau = x/U$ denotes the travel time between source and control plane. In the sub-
 384 sequent sections, we will account for the uncertainty in τ in order to derive a simple
 385 expression for the concentration probability density function (pdf) and λ is known.

5.2. Quantifying Probabilities of Occurrence

386 5.2.1. Probability of Travel Paths

387 Here we compute the probabilities of path 1 or 2 of occurring, i.e. events P_1 and P_2 (see
 388 Section 4 for definitions). We prefer to calculate the probability of the plume bypassing
 389 the control plane ($Pr[P_1]$). Since $Pr[P_1]$ and $Pr[P_2]$ are mutually exclusive, we have:

$$Pr[P_2] = 1 - Pr[P_1]. \quad (14)$$

390 In order to compute the above probabilities, we must quantify the pdf of each contami-
 391 nant particle within the source zone intercepting the control plane of the protection zone.
 392 Neglecting pore-scale dispersion (both longitudinal and transverse), we approximate the
 393 time of interception t_b by the mean travel time $t_b \approx \frac{L_b - L_s}{U}$ (time from the source to the
 394 control plane). In analogy to the work presented in *Bolster et al.* [2009], we assume a
 395 Gaussian model to describe the particle displacement pdf. For alternative definitions of
 396 the displacement pdf, we refer to *Dagan* [1987]; *Rubin* [2003]. Our resulting pdf is given
 397 by:

$$p_1(L_b, t_b) = \frac{1}{\sqrt{4\pi D_{\text{eff}} t_b}} e^{-\frac{(y_b - y_o)^2}{4D_{\text{eff}} t_b}}, \quad (15)$$

where y_o is a point within the contamination zone. D_{eff} is an effective macroscopic dispersion coefficient (purely uncertainty-related) that can arise for a variety of reasons, e.g., due to heterogeneity [Dagan, 1989; Rubin, 2003] or due to temporal fluctuations in the flow field [Dentz and Carrera, 2005] to mention but a few. Accounting for a dispersive term in Eq. (15), but not in Eq. (13), might seem inconsistent at first sight, but it is a consistent set of worst-case assumptions.

If no particles from the source bypasses the control plane either on the left or on the right, then no interception occurs. A conservative envelope can be constructed by considering that particles from the back right point [$\mathbf{s}_R = (L_s, y_{sR})$], see Figure 4, have to pass by the outer left point of the protection zone [$\mathbf{b}_L = (L_b, y_{bL})$] and vice-versa.

$$\begin{aligned} Pr(P_1) &= Pr(P_{1,L}) + Pr(P_{1,R}) \\ &= \int_{-\infty}^{y_{bL}} \frac{1}{\sqrt{4\pi D_{\text{eff}} t_b}} e^{-\frac{(y_b - y_{sR})^2}{4D_{\text{eff}} t_b}} dy_b \\ &\quad + \int_{y_{bRy}}^{\infty} \frac{1}{\sqrt{4\pi D_{\text{eff}} t_b}} e^{-\frac{(y_b - y_{sL})^2}{4D_{\text{eff}} t_b}} dy_b. \end{aligned} \quad (16)$$

5.2.2. Probability of Natural Attenuation

Above, we used the back end of the source as worst case scenario for interception with the protection zone. The worst case scenario for natural attenuation is based on the front center of the source area because this yields the shortest distance (thus shortest time) for decay.

413 Given the uncertainty in flow parameters and scarce site characterization, we con-
 414 sider for illustration the travel time τ to be stochastic and lognormally distributed [e.g.,
 415 *Cvetkovic et al., 1992*]:

$$f_{\tau}(\tau) = \frac{e^{-\frac{(\log(\tau) - \mu_{\tau})^2}{2\sigma_{\tau}^2}}}{\sqrt{2\pi}\sigma_{\tau}\tau}, \quad (17)$$

416 with μ_{τ} and σ_{τ} denoting the travel time mean and variance in logarithmic space and are
 417 related to the mean velocity [e.g., *Andricevic et al., 1994*].

We can now calculate the pdf for concentration based on the travel time pdf and Eq.
 (13):

$$f_c(C) = \left| \frac{d\tau}{dC} \right| f_{\tau}(\tau), \quad (18)$$

which allows us to evaluate the probability of the concentration being above a regulatory
 threshold value C_{crit} at the sensitive target. Substituting Eq. (13) into Eq. (18), we
 obtain:

$$f_c(C) = \frac{1}{\lambda C} f_{\tau} \left(\frac{1}{\lambda} \ln \left[\frac{C}{C_o} \right] \right), \quad (19)$$

418 Eq. (18) reflects only one possible and simple choice of model for the concentration pdf
 419 under the conditions assumed in the current work for illustrative purposes. It is worth
 420 mentioning that many other models could be used in this approach under more generic
 421 conditions [e.g., *Rubin et al., 1994; Bellin and Tonina, 2007; Cirpka et al., 2008*]. For
 422 example, other choices for travel time distributions can be found in Ch. 10 of *Rubin*
 423 [2003] and in *Sanchez-Vila and Guadagnini* [2005]. If hydrogeological data is available,
 424 one could also follow the approach described in *Rubin and Dagan* [1992] to condition the
 425 travel time pdf.

426 5.2.3. Probability of Risk Exceedence

427 Based on Eq. (5), we can evaluate the probability that the risk will exceed a threshold
 428 value r_{crit} . Here, we present a risk distribution for the commonly used risk model given
 429 in Eq. (2). In order to evaluate the risk cdf (F_R) based on the pdf f_β of the health
 430 parameters and concentration pdf f_C we have:

$$F_R(r_{crit}) = \int_0^{r_{crit}} \int_0^\infty f_\beta(\beta) f_C\left(\frac{r}{\beta}\right) \frac{1}{\beta} dr d\beta \quad (20)$$

431 where we used statistical independence between β and C . The concentration pdf comes
 432 from Eq. (18) while f_β is determined from population studies [e.g., *Dawoud and Purucker,*
 433 1996] or the data provided in *Maxwell et al.* [1998] and *Benekos et al.* [2007]. If a single
 434 individual with characteristics β_o is exposed, then Eq. (20) becomes:

$$\begin{aligned} F_R(r_{crit}) &= \int_0^{r_{crit}} \int_0^\infty \delta(\beta - \beta_o) f_C\left(\frac{r}{\beta}\right) \frac{1}{\beta} dr d\beta \\ F_R(r_{crit}) &= \frac{1}{\beta_o} \int_0^{r_{crit}} f_C\left(\frac{r}{\beta_o}\right) dr, \end{aligned} \quad (21)$$

435 where we used the properties of the Dirac Delta δ : $f_\beta(\beta) = \delta(\beta - \beta_o)$. This feature is
 436 incorporated in the fault tree represented in Figure 3 and illustrates how the approach can
 437 be used to cover cases for a single exposed individual and for a fully exposed population
 438 (also different population cohorts: gender and/or age dependent).

6. Results and Discussion

439 We illustrate the methodology by considering a simple example for cancer risk. Two
 440 species (A and B) are continuously released from their source locations and may pose
 441 a threat to human lives. The two contaminants are released in different locations, with
 442 different source dimensions and initial concentrations (to reproduce the varying range of

443 typical situations found in the field). Both contaminants are released from line sources
444 with dimensions 4 m (for contaminant A) and 2 m (for contaminant B). Contaminant A
445 is closer to the protection zone (35 m) while contaminant B is further away (60 m). These
446 values as well as other relevant parameters are summarized in Table 1. The main sources
447 of uncertainty under consideration here are the contaminant travel times, Eq. (17). We
448 also account for the variability in the health-related parameter β , Eq. (3). For the current
449 scenario, we assume that travel time standard deviation is equal to $\sigma_\tau = 0.1$ d and that
450 $D_{\text{eff}} = 0.1$ m²/d.

451 Since we have two distinct contaminants, the values for β are different. For instance,
452 contaminant A affects a specific population cohort while contaminant B affects a different
453 one (thus reflecting variability). In this example, we assume both values of β to be
454 lognormally distributed with mean $\mu_{\ln\beta}$ and standard deviation $\sigma_{\ln\beta}$, see Table 1 (values
455 given in logarithmic space). Figure 5 illustrates the pdf of β for contaminants A and B.
456 Risk estimates were obtained using the linear model in Eq. (2) and their corresponding
457 probabilities of exceeding a regulatory value are computed through the cdf provided in
458 Eq. (20).

459 Given that contamination is known to exist (*SO* with probability 1), we need to evaluate
460 the probabilities associated with each branch of the fault tree using the steps described
461 in Section 4. The events and their corresponding probabilities are summarized in Table 2
462 for both contaminants.

463 With the data given in Table 1 and using Eq. (16), the probability of the plume
464 hitting the sensitive target is $Pr[P_2] = 0.38$ for contaminant A and $Pr[P_2] = 0.26$ for
465 contaminant B. From the results given in Figure 6, we can also extract the probabilities

466 of the concentration being above a regulatory threshold value C_{crit} . The probabilities of C
 467 $\geq C_{crit}$ for contaminant A is 0.18 where for contaminant B we have 0.015. This is caused
 468 by the physical setup of the problem, since the source for contaminant A is closer to the
 469 environmentally sensitive target than to the release location of contaminant B. This shows
 470 how the extension of the contaminant source as well as its distance from the protection
 471 zone influences the probabilities of the plume hitting the target and of the concentration
 472 exceedance.

473 Figure 7 depicts the risk cdfs for both contaminants. Assuming that the critical risk
 474 value established by the regulatory agency is $r_{crit} = 10^{-4}$, we can compute the risk ex-
 475 ceedance probabilities $Pr(R > r_{crit})$ using Eq. (5), and obtain 0.69 and 0.54 for species
 476 A and B respectively. With Eq. (10), the probability of system failure can be obtained
 477 (values given in Table 2).

478 Next, we illustrate a sensitivity analysis to identify which parameters are more relevant
 479 in predicting the system failure for contaminants A and B. In addition, it serves as a first
 480 screening tool to see which parameters are dominant in each of the branches of the fault
 481 tree and may require more detailed investigation. The parameters chosen to perform the
 482 sensitivity analysis are $\theta = \{U, D_{eff}, \lambda, \sigma, \mu_{\ln\beta}, \sigma_{\ln\beta}\}$. We perturb, one by one, each
 483 parameter within θ by 10 percent and re-evaluate the probability of system failure each
 484 time. The resulting differences (between the perturbed and unperturbed case) given by
 485 $\Delta Pr[SF]$ are depicted in Figures 8 and 9 for contaminants A and B, respectively.

486 One striking difference between Figures 8 and 9 is the sensitivity of system failure to
 487 the health-related parameters: Contaminant A is more sensitive to the health-related
 488 parameters than contaminant B. This result aligns well with the results by *de Barros*

489 *and Rubin* [2008]. They showed that the relative significance of health-related parameters
490 decreases with travel distance, because of the uncertainty in transverse plume position
491 increases [*Rubin*, 1991]. Moreover, we note that both contaminants respond differently to
492 all other parameters, with the exception of the mean velocity.

493 For contaminant A, the macroscopic effective dispersion parameter (D_{eff}) is less impor-
494 tant, see Figure 8, since the source area for contaminant A is close to the environmental
495 target. Over short travel distances, the macroscopic effective dispersion has a small prob-
496 ability to make the plume bypass the protection zone (event P_2). Vice-versa, D_{eff} has
497 a larger significance in the probability of system failure for contaminant B, because its
498 source is located farther away from the target (event P_2).

499 The decay coefficient, λ , is the second most important parameter relative to the others
500 for contaminant A. Since the source for pollutant A is so close to the protection zone,
501 decay is the only process that can significantly reduce the probability of system failure.
502 The opposite occurs for contaminant B, since the significance of other events is higher.

503 Figure 10 shows how the coefficients of variation of the statistical distribution of risk
504 changes for each perturbation in θ . This quantifies how sensitive the uncertainty is in
505 assessing health risk to each individual parameter. In the current simple example, λ and
506 U have stronger effects on the uncertainty of risk for both species A and B than all other
507 parameters. We also observe that the mean and standard deviation of the health-related
508 component ($\mu_{\ln \beta}$ and $\sigma_{\ln \beta}$) has a significant contribution in the final risk pdf. These health
509 parameters have a stronger contribution to the spread of the risk pdf for contaminant A
510 (closer to the source) than for B. For predictions closer to the source, characterization
511 of the health parameters becomes important since concentrations are still high. As the

512 distance between the contaminant source and receptor increases, the contaminant plume's
513 peak concentration decreases due to the physical processes involved (in our case, decay).
514 Source dimensions and distance to the protection zone have a definite role in defining the
515 significance of the health parameters in the final risk. Again, this agrees with the results
516 from *de Barros and Rubin* [2008].

517 Although we have used a simple linear dose-response curve to evaluate cancer risk for
518 the illustration, many other alternatives exist with varying levels of uncertainty. For
519 instance, the work of *Yu et al.* [2003] provides detailed epidemiological dose-response
520 curves and parameter uncertainties for arsenic that are age- and gender-dependent. Such
521 dose-response curves are less subject to uncertainty than cancer risk models, because the
522 latter rely on extrapolated animal-to-human data. This implies that, if the a contaminant
523 site has several contaminants, different types of risk models could be used. This would lead
524 to different relative contributions to uncertainty propagation in assessing system failure
525 as discussed in *de Barros et al.* [2009].

526 An important and attractive feature of the methodology shown is that it allows one to
527 observe, in a most graphical manner, the sensitivity of the probabilities in system failure
528 for each branch of the tree. This is a crucial basis for supporting managing decisions. For
529 example, it indicates how to allocate resources towards further site characterization via
530 prioritization according to highest risk contributions and highest sensitivity.

7. Summary and Conclusions

531 In this work, we used the fault tree methodology to evaluate human health risk in a
532 probabilistic manner. The approach breaks complex problems into individual events that
533 can be tackled individually. The main differences between the ideas proposed here and the

534 previous works [*Tartakovsky, 2007; Winter and Tartakovsky, 2008; Bolster et al., 2009*]
535 are:

- 536 1. The fault tree proposed here accounts for the uncertainty in both hydrogeological
537 and health component;
- 538 2. System failure is defined in terms of risk being above a threshold value;
- 539 3. We introduced of a new form of stochastic fault-tree that weakens the assumption
540 of independent events which is necessary in conventional fault tree analysis.

541 Although we used only a crude and simple setting to illustrate the methodology, the
542 approach can be used with arbitrarily more complex models. However, such simple ap-
543 proaches can be useful for performing a preliminary screening in PRA, see works by
544 *Troldborg et al. [2008, 2009]*. For instance, with an initial estimate based on simple mod-
545 els, one can identify the events which contribute most to the final risk estimate or those
546 that propagate the highest degree of uncertainty throughout the system. This information
547 can then be used to invest further resources to these specific events, and more elaborate
548 models can be used if additional data becomes available. The divide & conquer and mod-
549 ularity features of the proposed framework easily allow the methods or tools used in each
550 component to be easily exchanged (and refined) in later analysis without being intrusive
551 in other components.

552 Moreover, assessing health-related risk in hydrosystems is an interdisciplinary field and
553 it relies on the expertise from a large number of disciplines (for example, hydrologists,
554 engineers, public health, etc). As a result, communicating the information across inter-
555 faces between different fields in an efficient and comprehensible manner is needed such
556 that reliable water management decisions are made. The divide and conquer approach

557 inherent to fault trees allows individual experts to work on the individual problems with
558 clear communication interfaces given by the fault tree structure. The approach allows
559 decision makers to better visualize the components culminating in system failure (e.g.,
560 population at risk) as well as the uncertainty emerging from each subsystem. This is
561 appealing from the decision maker's perspective, since it does not require entering into
562 the complex details of each component of the PRA and helps communicate probabilistic
563 concepts to practitioners. Furthermore, it acts as a translator to experts from different
564 fields, thus aiding public authorities in policy making and water management.

565 Despite the fact that our work focused on a groundwater contamination application,
566 it can be also used in other problems such as soil contamination, well vulnerability and
567 surface waters and catchment-scale coupled problems [e.g., *Frind et al.*, 2006; *Baresel and*
568 *Destouni*, 2007; *Troldborg et al.*, 2008, 2009; *Persson and Destouni*, 2009]. Furthermore,
569 an emerging challenge consists in using the ideas discussed in this paper to tackle a fully
570 integrated hydrosystem (groundwater, soil, surface water, etc.) where the need for divid-
571 ing a complicated problem into smaller ones as well as interdisciplinary communication
572 are even more evident [*Persson and Destouni*, 2009; *McKnight et al.*, 2010]. For instance,
573 *Bertuzzo et al.* [2008] studied how river networks (acting as environmental corridors) af-
574 fect the spreading of cholera epidemics. These authors clearly showed how hydrological,
575 health and demographical data needs to be considered in order to capture an accurate
576 description of the main controlling factors dictating the spread of cholera epidemics.

577 As pointed out in the literature, practitioners are still reluctant to embrace the concepts
578 of uncertainty [*Pappenberger and Beven*, 2006]. Such resistance has also been a matter
579 of discussion in a 2004 Forum published in *Stochastic Environmental Research and Risk*

580 *Assessment* [Christakos, 2004; Freeze, 2004; Rubin, 2004]. A common conclusion is that
581 the dialogue between the interdisciplinary groups is of utmost importance. Thus, having a
582 tool that allows to illustrate, in a rather simplistic manner, these concepts (uncertainties)
583 and its impact on society (for example, through risk) provides a step towards strengthening
584 the bridge between the scientific developments in stochastic hydrogeology and the state-
585 of-practice.

586 **Acknowledgments.** The first and fourth authors would like to thank the German
587 Research Foundation (DFG) for financial support of the project within the Cluster of
588 Excellence in Simulation Technology (EXC310/1) at the University of Stuttgart. This
589 work has been partially supported by the Spanish Ministry of Science and Innovation
590 through projects RARA AVIS (reference CGL2009-11114) and Consolider-Ingenio 2010
591 (ref. CSD2009-00065). We also would like acknowledge the comments made by our
592 reviewers.

References

- 593 Andricevic, R., and V. Cvetkovic (1996), Evaluation of Risk from Contaminants Migrating
594 by Groundwater, *Water Resources Research*, 32(3), 611–621.
- 595 Andricevic, R., J. Daniels, and R. Jacobson (1994), Radionuclide migration using travel
596 time transport approach and its application in risk analysis, *Journal of Hydrology*, 163,
597 125–145.
- 598 Baresel, C., and G. Destouni (2007), Uncertainty-accounting environmental policy and
599 management of water systems, *Environ. Sci. Technol*, 41(10), 3653–3659.

- 600 Bedford, T., and R. Cooke (2003), *Probabilistic Risk Analysis: Foundations and Methods*,
601 Cambridge University Press.
- 602 Bellin, A., and Y. Rubin (1996), HYDRO_GEN: A spatially distributed random field
603 generator for correlated properties, *Stochastic Hydrology and Hydraulics*, 10(4), 253–
604 278.
- 605 Bellin, A., and D. Tonina (2007), Probability density function of non-reactive solute con-
606 centration in heterogeneous porous formations, *Journal of contaminant hydrology*, 94(1-
607 2), 109–125.
- 608 Benekos, I., C. A. Shoemaker, and J. R. Stedinger (2007), Probabilistic risk and uncer-
609 tainty analysis for bioremediation of four chlorinated ethenes in groundwater, *Stochastic
610 Environmental Research Risk Assessment*, 21, 375–390.
- 611 Benson, D. A., and M. M. Meerschaert (2008), Simulation of chemical reaction via particle
612 tracking: Diffusion-limited versus thermodynamic rate-limited regimes, *Water Resour.
613 Res.*, 44, W12,201, doi:10.1029/2008WR007,111.
- 614 Bertuzzo, E., S. Azaele, A. Maritan, M. Gatto, I. Rodriguez-Iturbe, and A. Rinaldo
615 (2008), On the space-time evolution of a cholera epidemic, *Water Resources Research*,
616 44(1), 1–W01,424.
- 617 Bogen, K. T., and R. C. Spear (1987), Integrating Uncertainty and Interindividual Vari-
618 ability in Environmental Risk Assessment, *Risk Analysis*, 7(4), 427–436.
- 619 Bolster, D., M. Barahona, M. Dentz, D. Fernandez-Garcia, X. Sanchez-Vila, P. Trinchero,
620 C. Valhondo, and D. Tartakovsky (2009), Probabilistic risk analysis of groundwater
621 remediation strategies, *Water Resources Research*, 45(6).

- 622 Bolster, D., D. A. Benson, T. LeBorgne, and M. Dentz (2010), Anomalous mixing and
623 reaction induced by super-diffusive non-local transport, *Physical Review E*, *Submitted*.
- 624 Burmaster, D., and A. Wilson (1996), An introduction to second-order random variables
625 in human health risk assessments, *Human and Ecological Risk Assessment: An Inter-*
626 *national Journal*, *2*(4), 892–919.
- 627 Christakos, G. (2004), A sociological approach to the state of stochastic hydrogeology,
628 *Stochastic Environmental Research and Risk Assessment*, *18*(4), 274–277.
- 629 Cirpka, O., R. Schwede, J. Luo, and M. Dentz (2008), Concentration statistics for mixing-
630 controlled reactive transport in random heterogeneous media, *Journal of contaminant*
631 *hydrology*, *98*(1-2), 61–74.
- 632 Cvetkovic, V., A. Shapiro, and G. Dagan (1992), A solute flux approach to transport
633 in heterogenous formations 2: Uncertainty Analysis, *Water Resources Research*, *28*(5),
634 1377–1388.
- 635 Dagan, G. (1987), Theory of Solute Transport by Groundwater, *Annual Review of Fluid*
636 *Mechanics*, *19*, 183–215.
- 637 Dagan, G. (1989), *Flow and Transport in Porous Formations*, Springer Verlag, Berlin.
- 638 Davison, A., G. Howard, M. Stevens, P. Callan, L. Fewtrell, D. Deere, and J. Bartram
639 (2005), Water Safety Plans Managing drinking-water quality from catchment to con-
640 sumer. Geneva: World Health Organisation, *Tech. rep.*, WHO/SDE/WSH/05.06.
- 641 Dawoud, E., and S. Purucker (1996), Quantitative Uncertainty Analysis of Superfund
642 Residential Risk Pathway Models for Soil and Groundwater: White Paper, *Tech. rep.*
- 643 de Barros, F. P. J., and Y. Rubin (2008), A Risk-Driven Approach for
644 Subsurface Site Characterization, *Water Resources Research*, *44*(W01414),

645 doi:10.1029/2007WR006,081.

646 de Barros, F. P. J., Y. Rubin, and R. Maxwell (2009), The concept of comparative in-
647 formation yield curves and its application to risk-based site characterization, *Water*
648 *Resources Research*, 45(W06401), doi:10.1029/2008WR007,324.

649 Dentz, M., and J. Carrera (2005), Effective solute transport in temporally fluctuating flow
650 through heterogeneous media, *Water Resources Research*, 41(8), W08,414.

651 Donado, L. D., X. Sánchez-Vila, M. Dentz, J. Carrera, and D. Bolster (2009), Multicom-
652 ponent reactive transport in multicontinuum media, *Water Resour. Res.*, 45, W11,402,
653 doi:10.1029/2008WR006,823.

654 Edery, Y., H. Scher, and B. Berkowitz (2009), Modeling bimolecular reactions and trans-
655 port in porous media, *Geophys. Res. Lett.*, 36, L02,407 doi:10.1029/2008GL036,381.

656 Fiori, A., I. Jankovic, G. Dagan, and V. Cvetkovic (2007), Ergodic transport through
657 aquifers of non-Gaussian log conductivity distribution and occurrence of anomalous
658 behavior, *Water Resources Research*, 43(9), W09,407.

659 Fjeld, R., N. Eisenberg, and K. Compton (2007), *Quantitative Environmental Risk Anal-*
660 *ysis for Human Health*, first ed., Wiley.

661 Freer, J., K. Beven, and B. Ambroise (1996), Bayesian estimation of uncertainty in runoff
662 prediction and the value of data: An application of the GLUE approach, *Water Re-*
663 *sources Research*, 32(7), 2161–2173.

664 Freeze, R. (2004), The role of stochastic hydrogeological modeling in real-world engi-
665 neering applications, *Stochastic Environmental Research and Risk Assessment*, 18(4),
666 286–289.

- 667 Frind, E. O., J. W. Molson, and D. L. Rudolph (2006), Well vulnerability: a quantitative
668 approach for source water protection, *Ground water*, 44(5), 732–742.
- 669 Gelhar, L. W., C. Welty, and K. Rehfeldt (1992), A critical review of data on field scale
670 disperion in aquifers, *Water Resour. Res.*, 28, 1955–1974.
- 671 Gramling, C., C. Harvey, and L. Meigs (2002), Reactive transport in porous media: A
672 comparison of model prediction with laboratory visualization, *Environ. Sci. Technol.*,
673 36, 2508–2514.
- 674 Kitanidis, P. (1994), The concept of the dilution index, *Water Resources Research*, 30(7),
675 2011–2026.
- 676 Kitanidis, P. K. (1995), Quasi-linear geostatistical theory for inversing, *Water Resour.*
677 *Res.*, 31(10), 2411–2419.
- 678 Levy, M., and B. Berkowitz (2003), Measurement and analysis of non-fickian dispersion
679 in heterogeneous porous media, *Journal of Contaminant Hydrology*, 64, 203–226.
- 680 Maddalena, R. L., and T. E. McKone (2002), Developing and Evaluating Distributions
681 for Probabilistic Human Exposure Assessments, *Tech. Rep. LBNL-51492*.
- 682 Maxwell, R., and W. Kastenberg (1999), Stochastic Environmental Risk Analysis: An
683 Integrated Methodology for Predicting Cancer Risk from Contaminated Groundwater,
684 *Stochastic Environmental Research Risk Assessment*, 13, 27–47.
- 685 Maxwell, R., S. Pelmulder, F. Tompson, and W. Kastenberg (1998), On the development
686 of a new methodology for groundwater driven health risk assessment, *Water Resources*
687 *Research*, 34(4), 833–847.
- 688 Maxwell, R., W. Kastenberg, and Y. Rubin (1999), A methodology to integrate site char-
689 acterization information into groundwater-driven health risk assessment, *Water Re-*

- 690 *sources Research*, 35(9), 2841–2885.
- 691 Maxwell, R., S. Carle, and A. Tompson (2008), Contamination, Risk, and Heterogeneity:
692 On the Effectiveness of Aquifer Remediation, *Environmental Geology*, 54, 1771–1786.
- 693 McKnight, U., S. Funder, J. Rasmussen, M. Finkel, P. Binning, and P. Bjerg (2010), An
694 integrated model for assessing the risk of TCE groundwater contamination to human
695 receptors and surface water ecosystems, *Ecological Engineering*, *In Press*.
- 696 McKone, T., and T. Bogen (1991), Predicting the uncertainties in risk assessment, *Envi-
697 ron. Sci. Technol.*, 25(10), 1674–1681.
- 698 McLucas, A. C. (2003), *Decision making: risk management, systems thinking and situa-
699 tion awareness*, Argos Press, Canberra, Australia.
- 700 Molin, S., and V. Cvetkovic (2010), Microbial risk assessment in heterogeneous aquifers:
701 1. Pathogen transport, *Water Resources Research*, 46(5 (W05518)).
- 702 Molin, S., V. Cvetkovic, and T. Stenstrom (2010), Microbial risk assessment in heteroge-
703 neous aquifers: 2. Infection risk sensitivity, *Water Resources Research*, 46(5(W05519)).
- 704 Morales, K. H., L. Ryan, T. L. Kuo, M. Wu, and C. J. Chen (2000), Risk of Internal
705 Cancers from Arsenic in Drinking Water, *Environmental Health Perspectives*, 108(7),
706 655–661.
- 707 Neuman, S. P., and D. M. Tartakovsky (2009), Perspective on theories of anoma-
708 lous transport in heterogeneous media, *Adv. Water Resour.*, 32(5), 670–680, doi:
709 10.1016/j.advwatres.2008.08.005.
- 710 Nowak, W. (2010), Measures of parameter uncertainty in geostatistical estimation and
711 design, *Mathematical Geosciences*, 42(2), 199–221.

- 712 Nowak, W., F. P. J. de Barros, and Y. Rubin (2010), Bayesian geostatistical design:
713 Optimal site investigation when the geostatistical model is uncertain, *Water Resour.*
714 *Res.*, *46*(W03535), doi:10.1029/2009WR008,312.
- 715 Pappenberger, F., and K. Beven (2006), Ignorance is bliss: Or seven reasons not to use
716 uncertainty analysis, *Water Resources Research*, *42*(5), W05,302.
- 717 Persson, K., and G. Destouni (2009), Propagation of water pollution uncertainty and risk
718 from the subsurface to the surface water system of a catchment, *Journal of Hydrology*,
719 *377*(3-4), 434–444.
- 720 Raje, D., and V. Kapoor (2000), Experimental study of bimolecular reaction kinetics in
721 porous media, *Environ. Sci. Technol.*, *24*, 1234–1239.
- 722 Rubin, Y. (1991), Prediction of tracer plume migration in heterogeneous porous media by
723 the method of conditional probabilities, *Water Resour. Res.*, *27*(6), 1291–1308.
- 724 Rubin, Y. (2003), *Applied Stochastic Hydrogeology*, first ed., Oxford Press.
- 725 Rubin, Y. (2004), Stochastic hydrogeology - challenges and misconceptions, *Stochastic*
726 *Environmental Research Risk Assessment*, *18*, 280–281.
- 727 Rubin, Y., and G. Dagan (1992), Conditional estimates of solute travel time in heteroge-
728 nous formations: impact of transmissivity measurements, *Water Resources Research*,
729 *28*(4), 1033–1040.
- 730 Rubin, Y., M. A. Cushey, and A. Bellin (1994), Modeling of transport in groundwater for
731 environmental risk assessment, *Stochastic Hydrol. Hydraul.*, *8*(1), 57–77.
- 732 Sanchez-Vila, X., and A. Guadagnini (2005), Travel time and trajectory moments of con-
733 servative solutes in three dimensional heterogeneous porous media under mean uniform
734 flow, *Advances in Water Resources*, *28*, 429–439.

- 735 Sidle, C. R., B. Nilson, M. Hansen, and J. Fredericia (1998), Spatially varying hydraulic
736 and solute transport characteristics of a fractured till determined by field tracer test,
737 Funen, Denmark, *Water Resour. Res.*, *34*, 2515–2527.
- 738 Silliman, S. E., L. Konikow, and C. Voss (1997), Laboratory experiment of longitudinal
739 dispersion in anisotropic porous media, *Water Resour. Res.*, *23*, 2145–2154.
- 740 Tartakovsky, D. (2007), Probabilistic risk analysis in subsurface hydrology, *Geophysical*
741 *Research Letters*, *34*(5), 5404.
- 742 Tartakovsky, D. M., and C. L. Winter (2008), Uncertain future of hydrogeology, *ASCE*
743 *J. Hydrologic Engrg.*, *13*(1), 37–39.
- 744 Troldborg, M., G. Lemming, P. Binning, N. Tuxen, and P. Bjerg (2008), Risk assessment
745 and prioritisation of contaminated sites on the catchment scale, *Journal of contaminant*
746 *hydrology*, *101*(1-4), 14–28.
- 747 Troldborg, M., P. Binning, S. Nielsen, P. Kjeldsen, and A. Christensen (2009), Unsaturated
748 zone leaching models for assessing risk to groundwater of contaminated sites,
749 *Journal of contaminant hydrology*, *105*(1-2), 28–37.
- 750 Ucinski, D. (2005), *Optimal measurement methods for distributed parameter system identification*, CRC.
- 752 USEPA (1989), Risk Assessment Guidance for Superfund Volume 1: Human Health Manual
753 (Part A), *Tech. Rep. Rep.EPA/540/1-89/002*.
- 754 USEPA (1991), Risk Assessment Guidance for Superfund Volume 1: Human Health Evaluation
755 (Part B), *Tech. Rep. Rep.EPA/540/R-92/003*.
- 756 USEPA (2001), Risk Assessment Guidance for Superfund: Volume III - Part A, Process
757 for Conducting Probabilistic Risk Assessment, *Tech. Rep. Rep.EPA 540/R-02/002*.

758 Winter, C., and D. Tartakovsky (2008), A reduced complexity model for probabilistic risk
759 assessment of groundwater contamination, *Water Resources Research*, 30(6), 2799–
760 2816.

761 Yu, W., C. Harvey, and C. Harvey (2003), Arsenic in groundwater in Bangladesh: a
762 geostatistical and epidemiological framework for evaluating health effects and potential
763 remedies, *Water Resources Research*, 39(6), 1146.

764 Zimmerman, D. A., et al. (1998), A comparison of seven geostatistically based inverse ap-
765 proaches to estimate transmissivities for modeling advective transport by groundwater
766 flow, *Water Resour. Res.*, 34(6), 1373–1413.

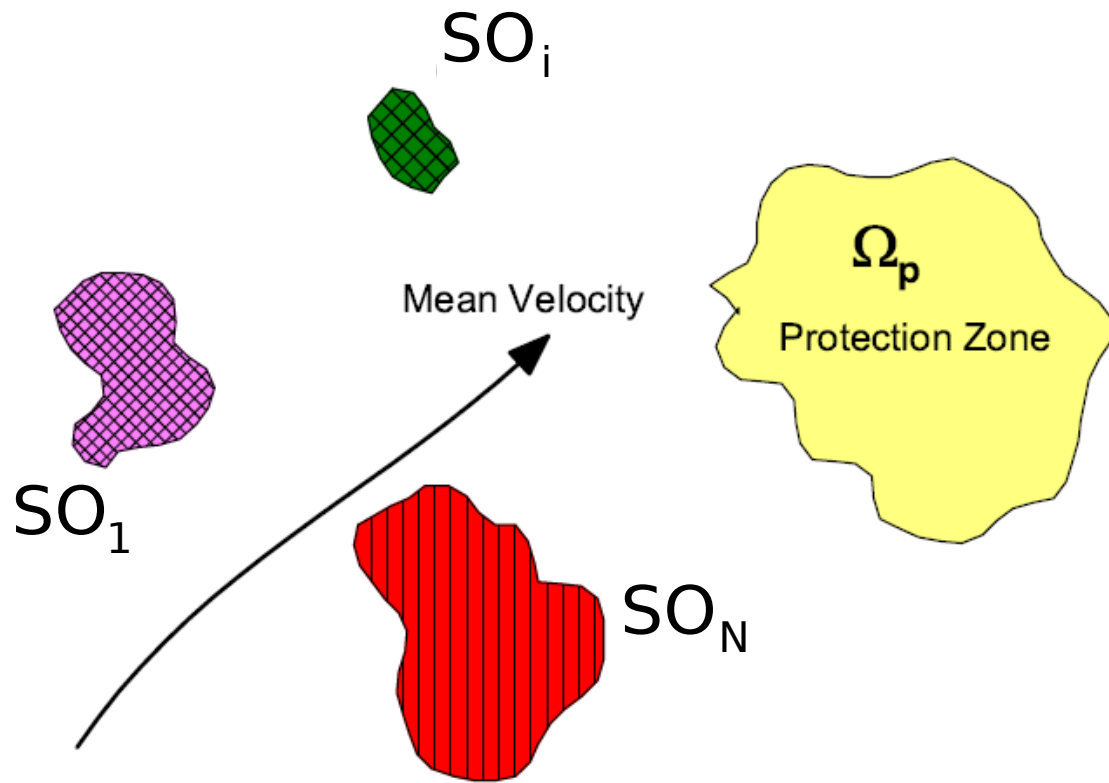


Figure 1. Schematic depiction of the contamination scenario considered in this work. Several potential sources SO_i , $i = 1, \dots, N$ are considered. Each source implies the combination of a potentially hazardous solute located in a given (sometimes unknown) location.

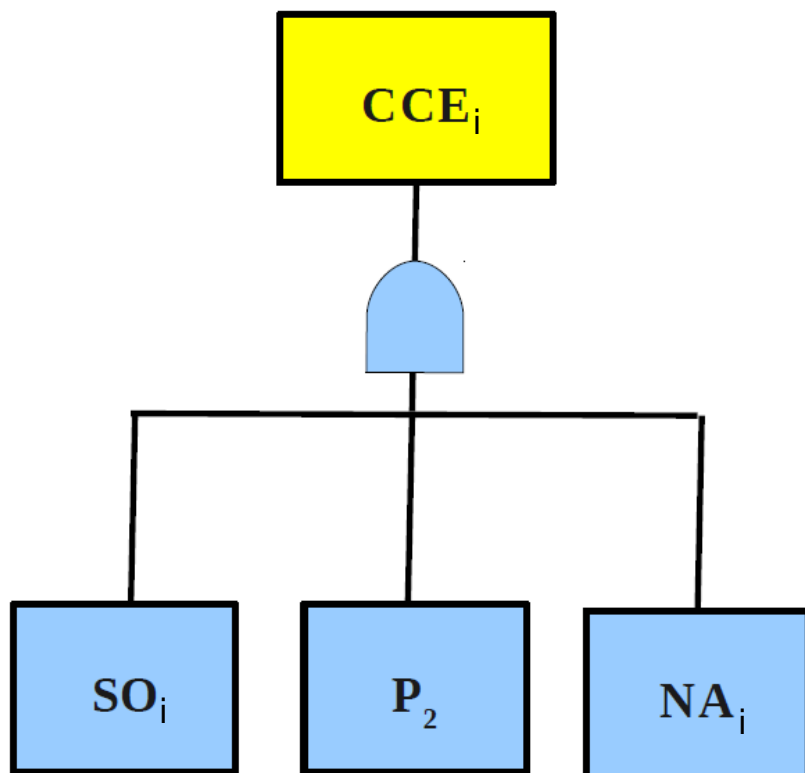


Figure 2. Fault tree for CCE_i .

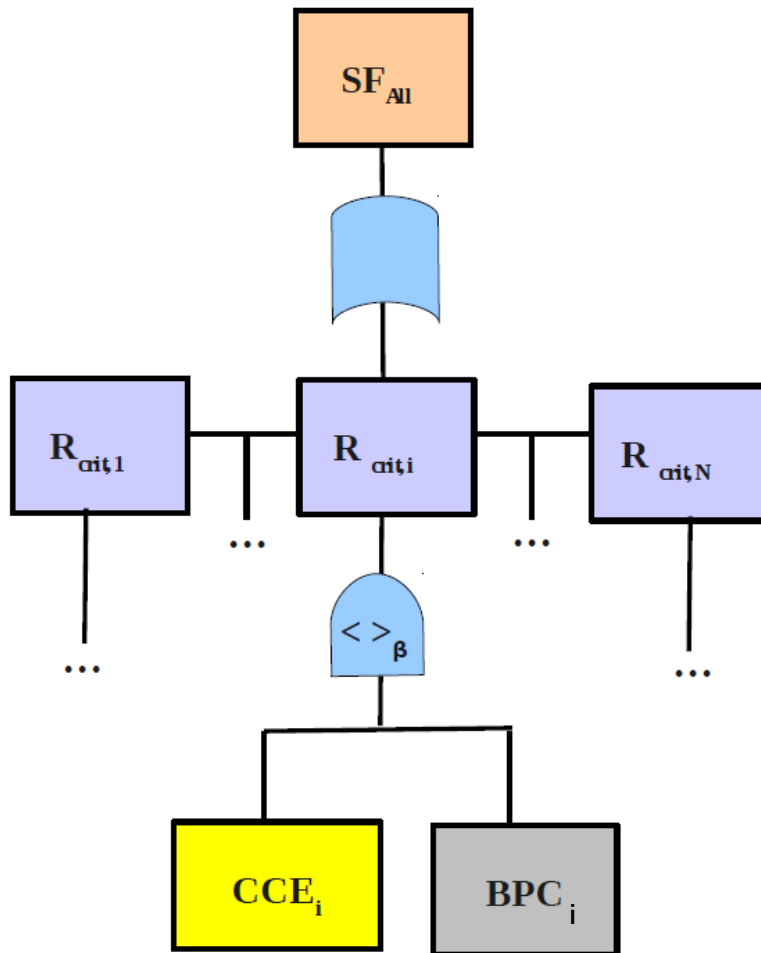


Figure 3. Fault tree for the total system failure

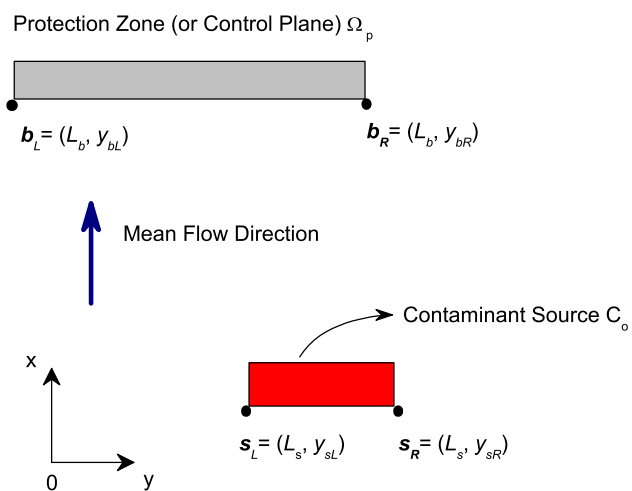


Figure 4. Schematic representation of the physical problem. A contaminant with initial concentration C_o is released. U is the mean velocity.

Data		
Parameter	A	B
C_o	1 mg/l	1.5 mg/l
λ	0.004 d ⁻¹	0.002 d ⁻¹
$L_b - L_s$	35 m	60 m
y_{sR}	12 m	4 m
y_{sL}	8 m	2 m
y_{bR}	1 m	1 m
y_{bL}	10 m	10 m
C_{cit}	0.1 mg/l	0.4 mg/l
$\mu_{\ln\beta}$	-5.54	-6.9
$\sigma_{\ln\beta}$	0.59	0.4

Table 1. Data for contaminant A and B.

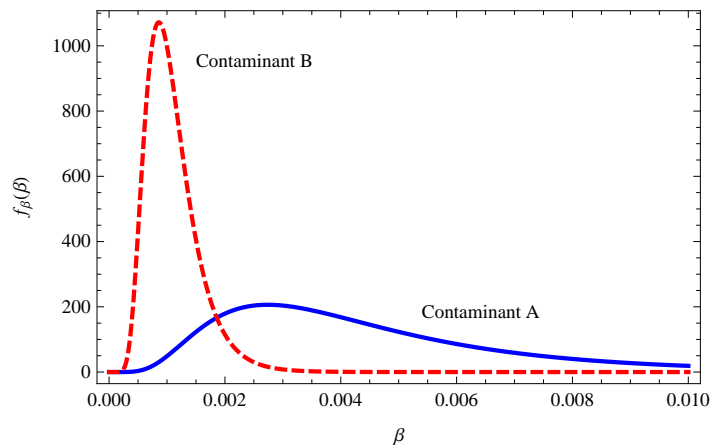


Figure 5. Distributions for the health-related parameters for contaminants A (continuous line) and B (dashed line).

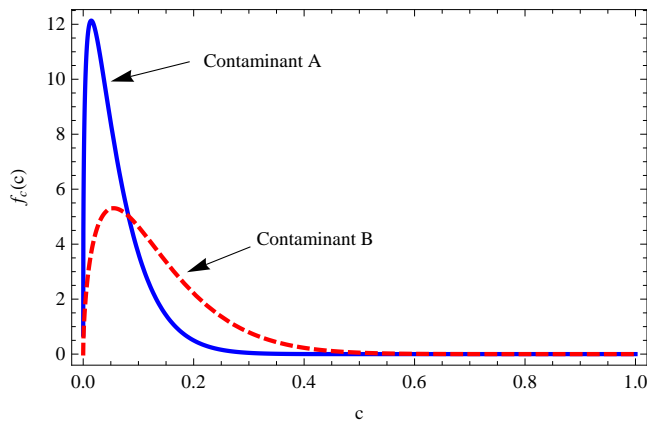


Figure 6. Concentration pdfs for contaminants A (continuous line) and B (dashed line) according to Eq. (18)

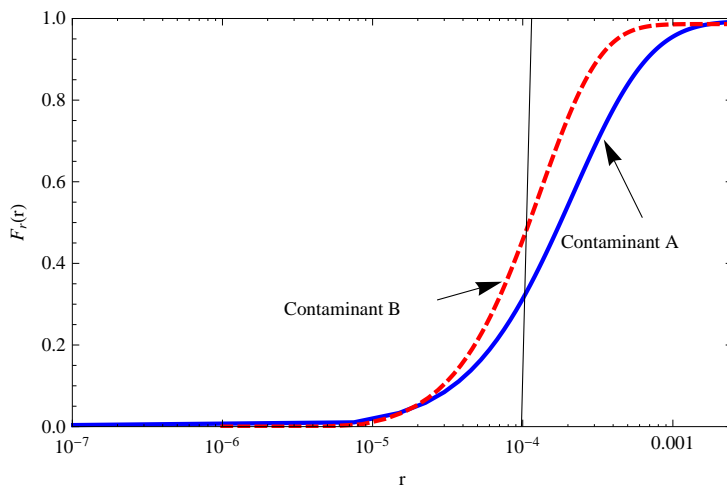


Figure 7. Risk cdf $F_r(r)$ for contaminants A (continuous line) and B (dashed line). The regulatory threshold is defined to be $r_{crit} = 10^{-4}$.

Probabilities			
Event	Parameter	A	B
SO	$Pr[SO]$	1	1
P_2	$Pr[P_2]$	0.38	0.26
NA	$Pr(C \geq C_{crit})$	0.18	0.015
R_{crit}	$Pr(r \geq R_{crit})$	0.69	0.54
SF	$Pr(SF)$	0.047	0.0022

Table 2. Computed probabilities for the hypothetical illustrative case

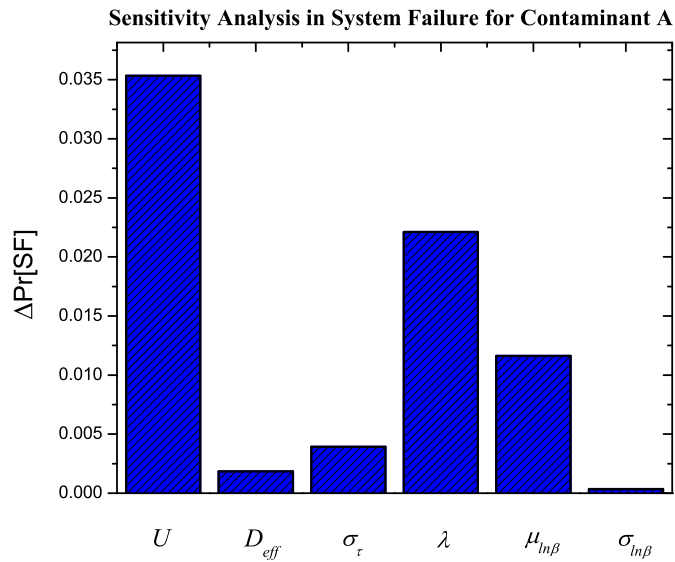


Figure 8. Sensitivity analysis for contaminant A. Change in probability of system failure $\Delta Pr[SF]$ if each parameter in θ is perturbed by 10 percent.

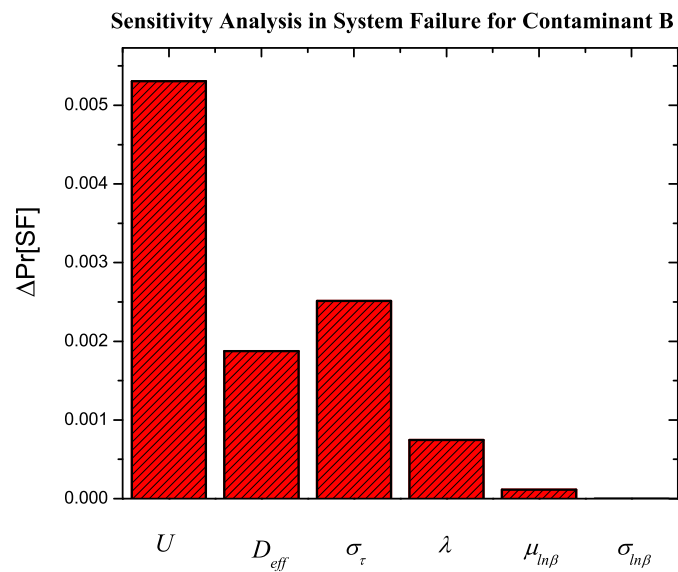


Figure 9. Sensitivity analysis for contaminant B. Change in probability of system failure $\Delta Pr[SF]$ if each parameter in θ is perturbed by 10 percent.

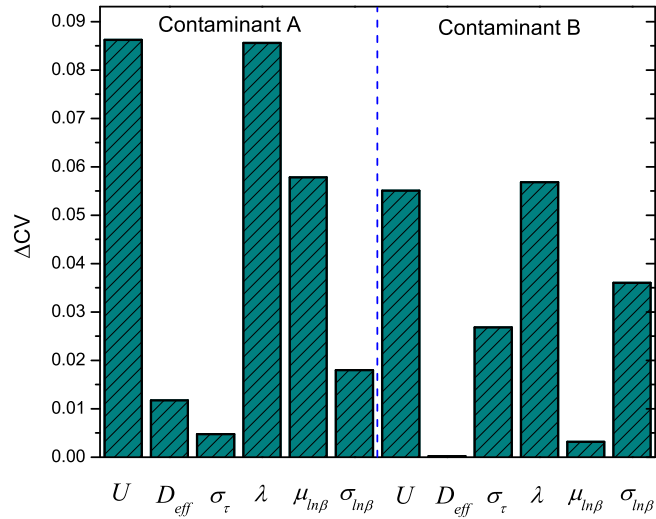


Figure 10. The dependency of the risk coefficient of variation for contaminants A and B on the perturbed parameter. Each parameter in θ was perturbed by 10 percent. The coefficient of variation is equal to the risk standard deviation divided by its mean. Results evaluated using Eq. 20. ΔCV corresponds to the change in the coefficient of variation.